environmental microbiology

Environmental Microbiology (2010) **12**(6), 1591–1603 doi:10.1111/j.1462-2920.2010.02199.x

The PhaD regulator controls the simultaneous expression of the *pha* genes involved in polyhydroxyalkanoate metabolism and turnover in *Pseudomonas putida* KT2442

Laura Isabel de Eugenio,[1‡] Beatriz Galán,[1‡] Isabel F. Escapa,[1] Beatriz Maestro,[2†] Jesús M. Sanz,[2] José Luis García[1] and María A. Prieto[1*]

[1]*Environmental Biology Department, Centro de Investigaciones Biológicas, CSIC, Ramiro de Maeztu, 9, 28040 Madrid, Spain.*

[2]*Instituto de Biología Molecular y Celular, Universidad Miguel Hernández, Av. Universidad, s/n. 03202 Elche, Spain.*

Summary

The promoters of the *pha* gene cluster encoding the enzymes involved in the metabolism of polyhydroxyalkanoates (PHAs) in the model strain *Pseudomonas putida* KT2442 have been identified and compared. The *pha* locus is composed by five functional promoters upstream the *phaC1*, *phaZ*, *phaC2*, *phaF* and *phaI* genes (P_{C1}, P_Z, P_{C2}, P_F and P_I respectively). P_{C1} and P_I are the most active promoters of the *pha* cluster allowing the transcription of *phaC1ZC2D* and *phaIF* operons. All promoters with the sole exception of P_F are carbon source-dependent. Their transcription profiles explain the simultaneous production of PHA depolymerase and synthases to maintain the metabolic balance and PHA turnover. Mutagenesis analyses demonstrated that PhaD, a TetR-like transcriptional regulator, behaves as a carbon source-dependent activator of the *pha* cluster. The *phaD* gene is mainly transcribed as part of the *phaC1ZC2D* transcription unit and controls its own transcription and that of *phaIF* operon. The ability of PhaD to bind the P_{C1} and P_I promoters was analysed by gel retardation and DNase I footprinting assays, demonstrating that PhaD interacts with a region of 25 bp at P_{C1} promoter (named OPRc1) and a 29 bp region at P_I promoter (named OPRi). These operators contain a single binding site formed by two inverted half sites of 6 bp separated by 8 bp which overlap the corresponding promoter boxes. The 3D model structure of PhaD activator predicts that the true effector might be a CoA-intermediate of fatty acid β-oxidation.

Received 3 November, 2009; accept 22 January, 2010. *For correspondence. E-mail auxi@cib.csic.es; Tel. (+34) 918 373 112; Fax (+34) 915 360 432. †Present address: Instituto Universitario de Electroquímica. Universidad de Alicante. 03080- Alicante, Spain. ‡Authors contribute equally to this work.

Introduction

The environmental pollution problems caused by the use of conventional plastics has generated a huge interest in the study of sustainable processes to generate these frequently used products from raw materials of agricultural or urban origins (Gavrilescu and Chisti, 2005). Some of the polyesters most seriously being considered as alternative plastics are the polyhydroxyalkanoates (PHAs). These are biodegradable polymers naturally produced by bacteria as carbon storage granules from renewable resources like glucose, fructose or fatty acids that form part of the vegetal oils (Madison and Huisman, 1999; Dias *et al.*, 2006; Prieto *et al.*, 2007). Medium-chain-length PHAs (mcl-PHA), containing 6–14 carbon atoms per monomer, are mainly produced by *Pseudomonas* species (Luengo *et al.*, 2003; Prieto *et al.*, 2007). Although bacterial fermentation and physicochemical characterization of the polymer have been studied extensively during the past few decades, knowledge on the molecular mechanisms regulating its synthesis and degradation is relatively limited (Prieto *et al.*, 1999; Hoffmann and Rehm, 2004; 2005; Sierro, 2005; Sandoval *et al.*, 2007). This is in part due to the complexity of PHA metabolism, which implies an extremely intricate regulatory system. Thus, PHA synthesis in Pseudomonads comprises: (i) central pathways, such as β-oxidation pathway and fatty acid *de novo* synthesis to convert fatty acid or carbohydrate intermediates, respectively, into different (*R*)-3-hydroxyalkanoyl-CoAs; and (ii) a specific or peripheral pathway encoded by the *pha* cluster including the genes encoding a depolymerase (PhaZ) (de Eugenio *et al.*, 2007; 2008; 2010) and two synthases (PhaC1 and PhaC2) (Huisman *et al.*, 1991), which coordinately with (iii) a granule-associated acyl-CoA-synthetase (Acs1) (Ruth *et al.*, 2008; Ren *et al.*, 2009), direct the carbon flux of these central metabolites towards PHA accumulation or hydrolysis as an active response to the carbon and

energy cellular demand (de Eugenio *et al.*, 2010; Ren *et al.*, 2009). It has been recently demonstrated in *Pseudomonas putida* KT2442 that PHA metabolism is an ongoing cycle where synthesis and degradation of the polyesters are simultaneously active facilitating the turnover of the polymer (de Eugenio *et al.*, 2010; Ren *et al.*, 2009). Besides the PHA related enzymes, formation and maintenance of PHA granules in the cytoplasm need the involvement of the major granule-associated proteins named phasins that play structural and regulatory roles (Prieto *et al.*, 1999).

The *pha* cluster is very well conserved among mcl-PHA producer strains (de Eugenio *et al.*, 2007; Prieto *et al.*, 2007) (Fig. 1). In addition to the two synthases and depolymerase coding genes, the cluster is composed by the *phaD* gene encoding a TetR-like transcriptional regulator (PhaD protein) (Klinke *et al.*, 2000; Ramos *et al.*, 2005) and the phasin-encoding *phaF* and *phaI* genes, which are transcribed divergently to the other *pha* genes (Prieto *et al.*, 1999; Moldes *et al.*, 2004; Sandoval *et al.*, 2007). PhaD plays an important role in mcl-PHA biosynthesis in *P. putida* GPo1 and its mutation affects polymer accumulation in several ways (Klinke *et al.*, 2000). In this sense, the mcl-PHA production was reduced in a *phaD*⁻ mutant and the number of PHA granules increased while size concomitantly decreased. Those effects have been ascribed to an altered expression of phasins (Klinke *et al.*, 2000; Sierro, 2005). Therefore, it has been suggested that PhaD is a transcriptional regulator which drives the expression of the PhaI and PhaF proteins (Sandoval *et al.*, 2007).

In this work, we have compared the activity of the promoter regions of the *pha* genes in the model strain *P. putida* KT2442. The role of PhaD as an activator of the *pha* cluster was demonstrated by mutagenesis analyses. Furthermore, the interaction of PhaD with their cognate promoters was studied by using gel retardation and DNase I footprinting analyses. Finally, the 3D structure of PhaD was modelled allowing us to predict that this protein might be activated by metabolic intermediates of the β-oxidation pathway of PHA precursors.

Results

Identification of promoter regions in the pha *gene cluster of* P. putida *KT2442: carbon source dependency*

The recent finding of a PHA turnover cycle due to the simultaneous activation of PHA synthase and depolymerase during growth of *P. putida* KT2442 (de Eugenio *et al.*, 2010) suggested that the expression of both genes might be coordinately regulated. To demonstrate this hypothesis we firstly identified the promoter regions driving the expression of the *pha* genes in *P. putida* KT2442. We constructed six *lacZ* promoter fusions with the upstream region of each *pha* gene (named P_{C1}, P_Z, P_{C2}, P_D, P_F and P_I promoter regions, Fig. 1), which were transferred into the chromosome of the wild-type strain by using the mini-transposon technique (a detailed description of DNA fragment sizes, primers used and plasmid constructions is shown in Table 1). The six isolated *P. putida* strains KTpC1, KTpZ, KTpC2, KTpD, KTpF and

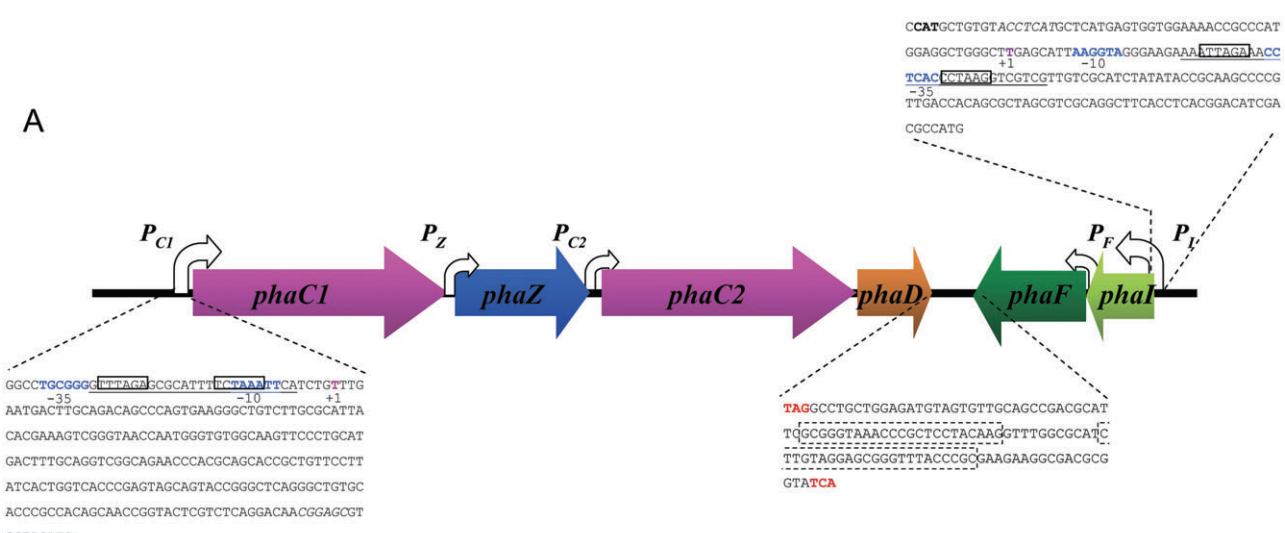

Fig. 1. Genetic organization of *pha* cluster, promoter sequences and intergenic regions in *P. putida* KT2442. The open arrows indicate the directions of gene transcription. P_{C1}, P_Z, P_{C2}, P_F and P_I are active promoter regions. The nucleotide sequences of the *phaD-phaF* intergenic region, 266 bp from P_{C1} promoter and 187 bp from P_I promoter are shown. The −35 and −10 boxes (blue) of the P_{C1} and P_I promoters and their transcription start sites (+1) (pink) are indicated. The DNA sequences corresponding to PhaD operators are underlined, with the inverted regions indicated in solid boxes. The REP sequences found between *phaD* and *phaF* genes in *P. putida* KT2442 are indicated in dashed boxes. Stop codons are marked in red. Translational start codons are indicated in bold letter.

Table 1. Construction of *lacZ* reporter *P. putida* KT2442 strains. Region amplified, fragment size, primers used, plasmid construction and resulting reporter strain.

Promoter region	Fragment size (bp)	Primers	Primers nucleotide sequence	pUJ9 derivative	pUTminiTn*5*-Km derivative	*P. putida* strain
P_{C1}	266	pC_15'	TTTGAATTCGGCCTGCGGGGTTTAGAG	pUJC1	pUTC1	KTpC1 (P_{C1}::*lacZ*)
		pC_13'	CGGGGATCCATCTACGACGCTCCGTTGT			
P_{C2}	242	pC_25'	TTTGAATTCCCCGTTGATCCCG	pUJC2	pUTC2	KTpC2 (P_{C2}::*lacZ*)
		pC_23'	CGCGGATCCATGGCAACACTCCCTCGTC			
P_Z	239	pZ5′	TTTGAATTCGACCCGGTGGCCTGGC	pUJZ	pUTZ	KTpZ (P_Z::*lacZ*)
		pZ3′	CGCGGATCCATGCACGTGACTCTTG			
P_D	737	pD5′	CCGGAATTCGCCACGTATCTGGTCAGCTTGC	pUJD	pUTD	KTpD (P_D::*lacZ*)
		pD3′	CGCGGATCCATCCAGTCAGCAGCTCATCGG			
P_F	219	pF5′	CCGGAATTCCCAGCTTGACGAAGTCGGTGA	pUJF	pUTF	KTpF (P_F::*lacZ*)
		pF3′	CGCGGATCCATCCTGCTCTCCTTATGGTTTGTG			
P_I	441	pI5′	CCGGAATTCGCCAGAAAATGCCTGAGAAGCTC	pUJI	pUTI	KTpI (P_I::*lacZ*)
		pI3′	CGCGGATCCATGCTGTGTACCTCATGCTC			

KTpI, carrying each *lacZ* fusion (Table 1), were cultured under PHA production conditions. The β-galactosidase activities were monitored in these strains at middle exponential phase (8 h) and at stationary phase (24 h) (Table 2). The main conclusion that can be drawn from these results was that under PHA production conditions functioned as promoter regions showing different expression levels. Conversely, no reporter activity was detected by this method when the strain *P. putida* KTpD (P_D::*lacZ*) was analysed. The highest level of reporter expression was detected in the strain *P. putida* KTpI carrying the P_I::*lacZ* fusion, which was more than 50-fold higher to that observed in KTpF and KTpC1 strains equipped with the P_F and P_{C1} reporter fusions respectively. Expression levels 5–10-fold lower than those found in KTpF and KTpC1 strains, were detected in cells carrying the P_Z::*lacZ* and P_{C2}::*lacZ* fusions. Our results also indicate that the expression level driven by each promoter, with the sole exception of P_F, was dependent of the carbon source supplied into the media (Table 2). The induction rate observed in the expression levels driven by the promoters P_{C1}, P_Z, P_{C2} and P_I when cells were cultured in octanoate versus glucose as preferred and poor PHA precursors, respectively, ranged from 1.5- to 2.5-fold higher (Table 2).

Table 2. β-Galactosidase activities of *lacZ* reporter *P. putida* KT2442 strains, PHA content and biomass concentrations.

Carbon source	*P. putida* strain	Time (h)	PHA content (%CDW)	Biomass (g l^{-1})	U βgal
Sodium octanoate	KTpI	8	33.3	1.12	7 974 ± 362
	KTpI	24	53.9	1.54	24 356 ± 684
	KTpF	8	32.7	1.23	181.9 ± 5.3
	KTpF	24	54.9	1.55	380.8 ± 2.3
	KTpD	8	30.0	0.99	ND
	KTpD	24	60.0	1.43	ND
	KTpC1	8	31.4	1.09	204.7 ± 2.9
	KTpC1	24	63.8	1.56	434.4 ± 4.6
	KTpC2	8	36.5	1.05	ND
	KTpC2	24	61.5	1.56	57.1 ± 1.8
	KTpZ	8	29.9	0.94	ND
	KTpZ	24	55.2	1.34	74.5 ± 2.2
Glucose	KTpI	8	< 5	0.62	581.9 ± 18.6
	KTpI	24	29.1	0.95	16 484 ± 438
	KTpF	8	< 5	0.61	380.3 ± 6.1
	KTpF	24	25.5	0.93	499.4 ± 12.2
	KTpD	8	< 5	0.67	ND
	KTpD	24	27.8	0.90	ND
	KTpC1	8	< 5	0.63	61.23 ± 3.5
	KTpC1	24	20.5	0.95	172.4 ± 1.0
	KTpC2	8	< 5	0.68	ND
	KTpC2	24	28.0	0.95	47.7 ± 1.0
	KTpZ	8	< 5	0.67	ND
	KTpZ	24	24.2	0.88	37.20 ± 2.6

ND, not detected.

Comparative quantification of pha *gene transcription rate by real-time RT-PCR*

Our results demonstrated that, with the exception of the putative *phaD* regulatory gene, the rest of the genes are preceded by a functional promoter region, and consequently, they might be transcribed independently responding to different physiological and PHA metabolic conditions. However, the absence of putative transcription terminators downstream the *phaC1*, *phaZ*, *phaC2* and *phaD* genes (Fig. 1) or between the phasin-coding genes *phaI* and *phaF*, indicated that the co-existence of a variety of polycistronic transcription units (operons) cannot be excluded. Consequently and to ensure the detection of all putative *pha* transcription units, the expression profile of the *pha* genes was comparatively monitored by real-time RT-PCR throughout the growth curve in the wild-type strain cultured in octanoate or glucose as preferred and poor PHA precursors respectively (see *Experimental procedures* for details). In agreement with the experiments performed with the *lacZ* reporter strains (Table 2), the transcription rate of all *pha* genes in the wild-type strain was optimal when the cells were cultured in the presence of octanoate, reaching in all cases a maximum level at exponential phase (7 h) (Table 3 and Fig. S1, see *Supporting information*). The transcription levels of the *phaF* and *phaI* genes were more that sevenfold higher than those of *phaC1* gene. These results are in agreement with the fact that phasins are the major proteins associated to the PHA granule (Moldes *et al.*, 2004).

Table 3. Quantification of the expression rates of the *pha* genes by real-time RT-PCR assays.

		Transcription level (cDNA ng $\times 10^3$)[a]	
P. putida strain	Gene	*Octanoate*	*Glucose*
KT2442	*phaC1*	2 654 ± 742	162 ± 57
	phaZ	996 ± 314	30.8 ± 13.6
	phaC2	639 ± 219	69.9 ± 17.8
	phaD	167 ± 47	33.0 ± 16.0
	phaF	21 089 ± 1 537	1 288 ± 308
	phaI	20 578 ± 4 882	879 ± 94
KT42C1	*phaC1*	ND[b]	ND[b]
	phaZ	5.4 ± 1.8	6.2 ± 5.4
	phaC2	14.7 ± 5.6	19.3 ± 5.2
	phaD	9.2 ± 4.2	8 ± 6.7
	phaF	869 ± 601	505 ± 34
	phaI	94.3 ± 12.1	43.4 ± 12.5
KT42D	*phaC1*	527 ± 178	86.3 ± 33.6
	phaZ	115 ± 64	38.7 ± 34.4
	phaC2	45 ± 24.4	42.5 ± 15.1
	phaD	729 ± 127	310 ± 106
	phaF	444 ± 35	312 ± 91
	phaI	ND[b]	ND[b]

a. Samples were taken 7 h after inoculation.
b. Not detected.

PhaD activator role on the P_{C1} *promoter*

Promoter activity quantification data derived from the *lacZ* reporter strains showed that P_{C1} is 10-fold more active than P_Z and P_{C2} (Table 2). However, the results obtained by the relative quantification of the *phaC1*, *phaZ* and *phaC2* mRNAs (Table 3 and Fig. S1) showed lower transcription rate differences suggesting that the expression of *phaC1*, *phaZ* and *phaC2* genes could be partially driven by the P_{C1} promoter directing the transcription of a polycistronic unit. Furthermore, the transcription rates of *phaC1*, *phaZ*, *phaC2* and *phaD* were inversely proportional to the distance from the P_{C1} promoter region suggesting as well that they were co-transcribed as an operon. Accordingly, the absence of promoter activity in the upstream region of the *phaD* gene suggested that the expression of this gene is controlled by an upstream promoter. To check this possibility, the expression of the *pha* genes was analysed in the *P. putida* KT42C1 (PhaC1$^-$) and KT42D (PhaD$^-$) mutant strains (Table 3 and Fig. S1). When *phaC1* was disrupted, the transcription levels of the other *pha* genes were severely affected (Table 3 and Fig. S1). Similar polar effects on the expression rate of *pha* genes were observed when *phaD* was interrupted (Table 3 and Fig. S1). The reduced transcription rate observed for the *phaC1*, *phaI* and *phaF* genes in the PhaD mutant can only be explained if PhaD protein works as an activator of the cognate promoters. With the sole exception of *phaI* gene, only basal expression levels were detected in the genes *phaC1*, *phaZ*, *phaC2* and *phaF*, in the KT42D (PhaD$^-$) mutant strain, suggesting that they are likely driven by the internal promoters P_Z, P_{C2} and P_F and a basal activity of the P_{C1} promoter.

These results clearly demonstrated that the integrity of the DNA region comprising *phaC1*, *phaZ*, *phaC2* and *phaD* is crucial for the efficient transcription of the whole *pha* gene cluster when cells were grown in octanoate as carbon and energy sources, suggesting the existence of the *phaC1ZC2D* operon where PhaD acts as an activator of the *pha* cluster. The expression level of *phaC1ZC2D* operon detected when the wild-type cells were cultured in glucose did not differ significantly from those detected in the KT42D (PhaD$^-$) mutant strain growing in octanoate, indicating that PhaD controls the carbon source dependence of the transcription profile of this operon and that the system might be induced either by octanoate or some octanoate-derived metabolite.

The PHA content data did proportionally reflect the lack of induction in the presence of octanoate. Then, PHA accumulation from octanoate was significantly affected but not abolished in the KT42D (PhaD$^-$) mutant strain after 24 h of culture [18 ± 2 PHA as % of cell dry weight (CDW)] when compared with the wild-type strain (70 ± 2 PHA as % of CDW). Thus, the existence of alternative

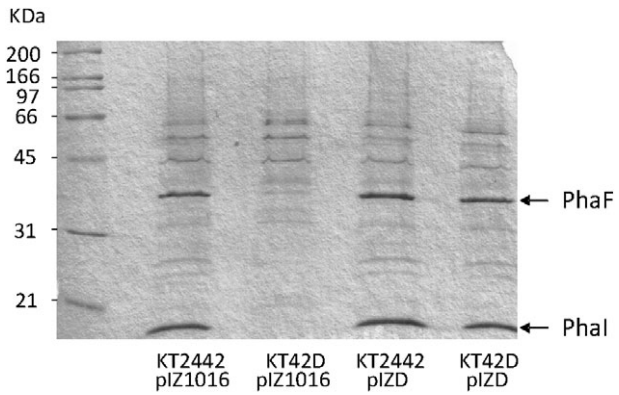

Fig. 2. Comparative analyses of granule-associated proteins from *P. putida* KT2442 and KT42D strains. Cells were grown under PHA production conditions for 24 h, and granules were isolated using a glycerol gradient centrifugation as described (de Eugenio *et al.*, 2007). Suspensions of granules were normalized at 150 optical units (OD_{650}). Samples of purified granules were mixed 1:1 (v/v) with sodium dodecyl sulfate-polyacrylamide gel electrophoresis (SDS-PAGE) loading buffer, and the bound proteins were separated by SDS-PAGE as described (Laemmli, 1970).

weak promoters (non-PhaD-induced P_{C1}, P_Z and P_{C2}) ensures the accumulation of the polymer under non-favourable conditions. In this sense, the KT42C1 (PhaC1$^-$) mutant is able to produce 0.5 $\pm$ 0.1 PHA as % of CDW (de Eugenio *et al.*, 2010), very likely due to a basal activity of the PhaC2 polymerase.

PhaD activates the P_I *promoter*

The PhaD protein of *P. putida* GPo1 and *P. putida* U has been proposed to act as a transcriptional regulator belonging to the TetR family of regulators, which activates the transcription of the *phaI* gene (Klinke *et al.*, 2000; Ramos *et al.*, 2005; Sandoval *et al.*, 2007). The experiments shown in Table 3 and Fig. S1 demonstrated that *phaI* mRNA is completely absent in the KT42D (PhaD$^-$) mutant strain and only a very weak expression was detected for the *phaF* gene (Fig. S1). In fact, the PhaI and PhaF phasins were not detected in the PHA granules when the KT42D (PhaD$^-$) cells were cultured under PHA production conditions in the presence of octanoate (Fig. 2). The pIZD plasmid expressing PhaD was able to restore the capacity of KT42D (PhaD$^-$) mutant to accumulate PHA (65 PHA as % CDW) at a similar ratio than the wild-type strain. As expected, the PHA granules of *P. putida* KT42D (pIZD) contained PhaI and PhaF as the major granule-associated proteins.

Taking together the RT-PCR results (Table 3 and Fig. S1), which showed constitutive levels of *phaF* mRNA in the absence (*P. putida* KT42D) or low levels (*P. putida* KT42C1) of PhaD protein, our findings confirm the crucial role of PhaD in the expression of the phasin-coding genes, and suggest the existence of a *phaIF* operon driven by the P_I promoter as well as a PhaD-independent expression of *phaF* driven by the P_F promoter. These results agree with those reported in *P. putida* GPo1, where a weak constitutive P_F promoter was proposed for the permanent production of the PhaF protein (Prieto *et al.*, 1999).

Characterization of the PhaD-operator regions at P_{C1} *and* P_I *promoters*

To demonstrate the direct implication of PhaD in the transcription driven by P_{C1} and P_I promoters and the PhaD-independent P_F activity, we analysed the ability of PhaD to bind the corresponding intergenic regions by gel retardation assays [electrophoretic mobility shift assay (EMSA)] using cell-free extracts from *Escherichia coli* DH10B (pIZD) and P_{C1}, P_I and P_F DNA fragments as probes respectively (Table 1, Fig. S2). While PhaD was able to retard the migration of both P_{C1}, and P_I probes in a protein concentration-dependent manner, the P_F probe did not, suggesting that PhaD is able to bind to P_{C1} and P_I promoters even in the absence of any inducer. Moreover, experiments with unrelated DNA from salmon sperm demonstrated that the PhaD binding to the P_I promoter region was highly specific (Fig. S2). On the other hand, the lack of PhaD binding to the P_F promoter region confirmed the existence of two transcription units in this region. Finally, to identify the inducer of PhaD protein, EMSAs were performed in the presence of PHA latex (2–20 μg, prepared as described in Schirmer and Jendrossek, 1994) and octanoate (0.1–1.0 mM) (see *Experimental procedures*). However, these compounds did not change the retardation pattern of the DNA probes (data not shown).

To precisely localize the PhaD operators and transcription start sites in the P_{C1} and P_I promoters, primer extension and DNase I footprinting analyses were performed using total RNA isolated from *P. putida* KT2442 and the P_{C1} and P_I probes respectively (Figs 1 and 3). The P_I promoter transcription initiation site was mapped 54 nucleotides upstream of the ATG translation initiation codon of the *phaI* gene, showing two −10 (TACCTT) and −35 (GTGAGG) putative boxes, which differ in three nucleotides from the consensus RpoD-dependent promoters (Fig. 1). A major transcription initiation site was located in the P_{C1} promoter 224 nucleotides upstream of the ATG translation initiation codon of the *phaC1* gene showing the −10 (TAAATT) and −35 (TGCGGG) putative boxes (Fig. 1).

DNase I footprinting experiments revealed that PhaD protects a region of 25 bp at P_{C1} promoter (named OPRc1) and a 29 bp region at P_I promoter (named OPRi) (Fig. 3). Both protected sequences contains a single binding site formed by two inverted half sites of 6 bp separated by 8 bp (Fig. 3C). Interestingly, OPRc1 and

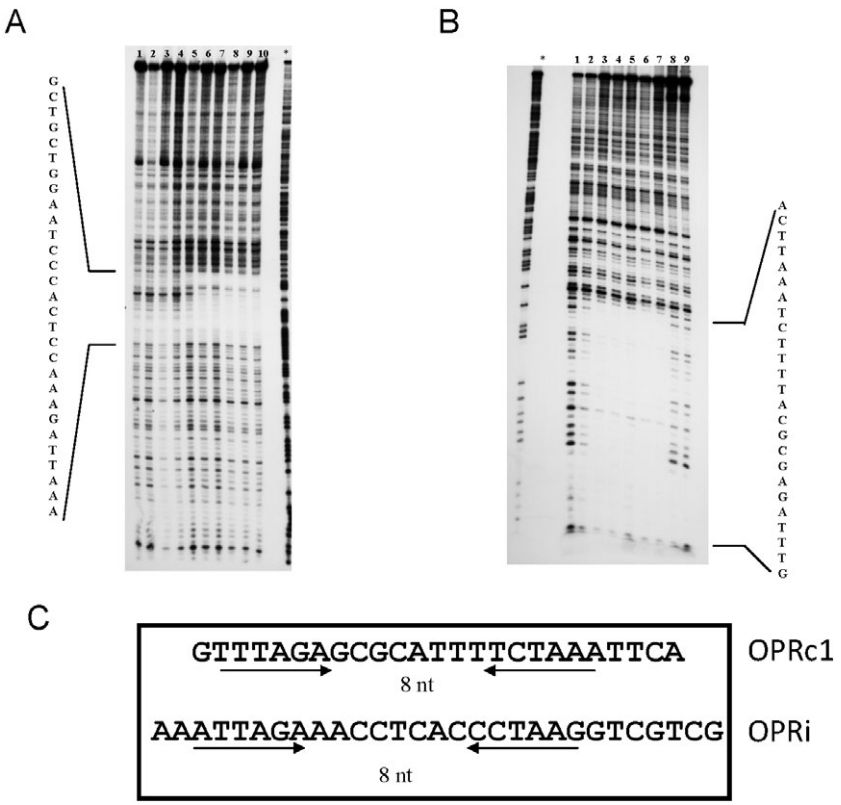

Fig. 3. Characterization of P_I and P_{C1} promoters.
A and B. DNase I footprinting analyses of PhaD interaction with the P_I and P_{C1} promoter regions respectively. The reaction mixture was treated as described in *Experimental procedures*, using the 5′-end-labelled non-coding strand and the 5′-end-labelled coding strand of the P_I and P_{C1} regions respectively. The A+G sequencing ladder is indicated with an asterisk.
A. Lanes 1 and 2: naked DNA; lanes 3 and 4 contain 0.6 and 6 μg of total protein of PhaD-free extracts obtained from *E. coli* cells bearing control plasmid pIZ1016 respectively, and lanes 5–10 contain 0.6, 1.2, 1.5, 2, 3 and 6 μg of total protein of PhaD+ extracts,
B. Lane 1, naked DNA; lanes 2–7 contain 0.6, 1.2, 1.5, 2, 3 and 6 μg of total protein of PhaD+ extracts and lanes 8 and 9 contain 0.6 and 6 μg of total protein of PhaD-free extracts obtained from cells bearing control plasmid pIZ1016 respectively.
C. Sequences of the PhaD-binding sites at P_I and P_{C1} promoters. The palindromic sequences are indicated by inverted black arrows.

OPRi operators overlap the promoter boxes in their cognate promoter regions suggesting a similar regulatory mechanism of the PhaD protein.

Homology modelling of PhaD

PhaD controls the carbon source dependence of the transcription profile of the *pha* cluster and this regulatory system seems to be induced by a metabolite derived from fatty acid β-oxidation pathway. To get insight into the structural basis supporting this hypothesis, we modelled the 3D structure of the PhaD protein using the 3D structures of similar regulators belonging to the TetR family as templates (i.e. Schumacher *et al.*, 2001; 2002; Rajan *et al.*, 2006; Premkumar *et al.*, 2007). All these regulators show α-helical dimeric structures containing an N-terminal helix–turn–helix (HTH) DNA-binding domain, plus a C-terminal domain involved in dimerization and effector binding. Among the available templates, the structure of the EthR repressor from *Mycobacterium tuberculosis* complexed with hexadecyloctanoate (Frénois *et al.*, 2004) was especially attractive due to the similarity of this ligand with some of the putative PhaD effectors like hydroxyoctanoyl-CoA (HOCoA). The modelled PhaD structure predicts the existence of a dimer, being each monomer composed of two domains built up from nine α-helices (α1-9), where the α2 and α3 helices constitute a HTH motif in the N-terminal domain (Fig. 4). Helices α8 and α9 would be involved in dimerization through the configuration of a four-helix bundle. The most noteworthy feature of this model is the presence of a long, deep crevice surrounded by helices α5–α8 that spans the whole C-terminal domain (Fig. 4 and Fig. S3) and that is

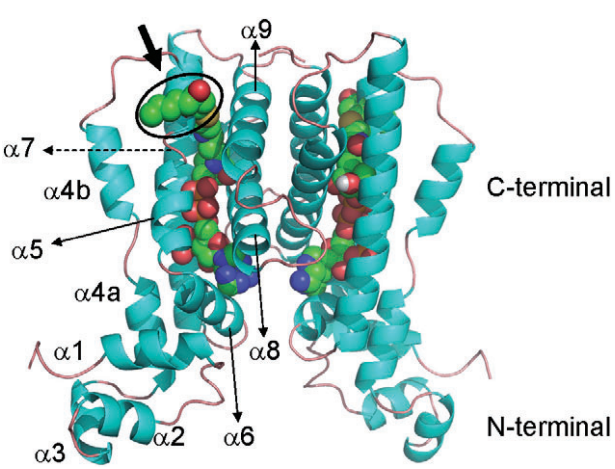

Fig. 4. Homology-based 3D model of dimeric PhaD.
Three-dimensional model based on the structure of EthR from *M. tuberculosis*. The protein is depicted in cartoon representation, and the HOCoA molecule is shown in spacefill format. Numbered α-helices are also shown. Oval and arrow highlight the 3-hydroxyoctanoyl moiety in HOCoA.

used in the case of EthR to bind its hexadecyloctanoate ligand. We observed that an elongated HOCoA molecule could also fit inside the crevice without sterical impediments and establish a number of stabilizing interactions with several amino acid side-chains (Fig. S3).

Discussion

To date, the transcriptional regulation of *pha* genes of *Pseudomonas* species has been scarcely studied and only incomplete and disperse information is available for some of the best-known PHA producer strains (reviewed in Prieto *et al*., 2007). In this work, we have identified the activity of the promoter regions of the *pha* genes in the model strain *P. putida* KT2442 and compared the activity of each individual promoter with the total mRNA generated for each *pha* gene. These experiments have allowed us to definitively determine that the *pha* locus in *P. putida* KT2442 is composed by at least five functional promoters upstream the *phaC1*, *phaZ*, *phaC2*, *phaF* and *phaI* genes (P_{C1}, P_Z, P_{C2}, P_F and P_I respectively), and that P_{C1} and P_I are the most active promoters in the *pha* cluster, allowing the transcription of *phaC1ZC2D* and *phaIF* operons. This transcription profile correlates with the simultaneous production of PHA depolymerase and synthases to maintain the metabolic balance and PHA turnover (de Eugenio *et al*., 2010). All promoters with the sole exception of P_F are carbon source-dependent. Octanoate, a PHA precursor carbon source, increased the transcription driven by these dependent promoters, while less preferred PHA precursor carbon sources, like glucose, caused lower levels of gene transcription. It is interesting to notice that the presence of weak promoters might allow the expression of specific *pha* genes under diverse physiological circumstances (see below). The most active promoter is P_I driving the expression of the *phaF* and *phaI* genes, which agrees with the major content of phasins in the PHA granules (Prieto *et al*., 1999; Moldes *et al*., 2004).

The *phaD* gene encoding a TetR-like transcriptional activator is mainly transcribed as part of the *phaC1ZC2D* transcription unit, although it could be also expressed from P_Z or P_{C2} promoters which can drive the alternative transcription units *phaZC2D* and *phaC2D* respectively. The results shown in Table 3 and Fig. S1 demonstrated that the carbon source-dependent induction of the *pha* genes is controlled by PhaD that is acting as an activator. However, the influence of the carbon source in the transcription profile of the *phaC1* and *phaZ* mRNAs was still detectable in the absence of PhaD mutant strain (KT42D) suggesting that additional factors might control the expression of the *pha* cluster (Table 3 and Fig. S1). In this sense, the PhaF phasin and some global transcriptional factors like the GacS/GacA system have been demonstrated to be involved in the regulation of *pha* gene expression (Prieto *et al*., 1999; Castaneda *et al*., 2000; Kessler and Witholt, 2001; Hoffmann and Rehm, 2004; Sandoval *et al*., 2007).

Pseudomonas putida KT2442 is able to accumulate PHA from glucose although at minor extend than from fatty acids (Huijberts *et al*., 1992) (Table 2) due to the presence of the specific PhaG transacylase that converts the (*R*)-3-hydroxyacyl-acyl carrier protein [(*R*)-3-hydroxyacyl-ACP)] intermediates of the fatty acid biosynthesis route into the substrate of the PHA synthase, i.e. the (*R*)-3-hydroxyacyl-CoA (Rehm *et al*., 1998). The lack of *pha* transcriptional activation when the strain grows in glucose suggests that the actual PhaD inducer might be an intermediate of the fatty acid β-oxidation pathway, which is only barely produced when cells are cultured in this carbon source. Nevertheless, in these circumstances the basal activities of the *pha* promoters still allow *P. putida* KT2442 to accumulate PHA.

Although the *pha* gene organization and gene products are highly conserved in the *P. putida* mcl-PHA producer strains, nucleotide sequences of *pha* cluster intergenic regions differ considerably among these strains (Kessler and Witholt, 2001; Solaiman *et al*., 2008). In fact, very recent studies about the *pha* clusters from the phylogenetically related strains *Pseudomonas corrugata* and *Pseudomonas mediterranea* show vastly differences in the *pha* intergenic regions (Solaiman *et al*., 2008). Consequently, it would be not surprising that transcriptional factors might trigger different effects in different PHA producer strains. Unlike in other bacteria, the *pha* locus in *P. putida* U seems to be integrated by six different functional units (*phaC1*, *phaZ*, *phaC2*, *phaD*, *phaI* and *phaF*) (Sandoval *et al*., 2007). In *P. putida* GPo1, two promoters have been reported upstream of the *phaC1* gene (P_{C1} region), showing transcriptional start sites at 198 and 112 bp upstream of the *phaC1* ribosomal binding site, respectively, being the later RpoN dependent (Huisman, 1991). On the other hand, there are at least two promoters involved in the expression of the *pha* genes in *Pseudomonas aeruginosa* that are located upstream of the *phaC1* gene and resemble the consensus sequences for RpoN and RpoD-dependent promoters (Timm and Steinbüchel, 1992). We have shown that the P_{C1} transcription start site in *P. putida* KT2442 lays at 224 bp upstream the ATG codon.

The mRNA analyses carried out in the GPo1 strain showed that all the transcripts were shorter than 3 kb, suggesting that *phaC1*, *phaZ*, *phaC2* and *phaD* do not form part of the same transcription unit, or that an mRNA processing event is taking place (Prieto *et al*., 1999). The existence of *phaC1* and *phaC1Z* transcription units was demonstrated in GPo1 as also reported for the homologous system of *P. aeruginosa* (Prieto *et al*., 1999; 2007). Thus, in *P. putida* GPo1 the transcription should partially

stop at the end of the *phaC1* gene and partially continue to the end of *phaZ*. This assumption is in agreement with the presence in this strain of a structure analogous to the enterobacteriaceae repetitive extragenic palindromic (REP) sequences located downstream of the *phaZ* gene, which might function as transcription terminator (Huisman *et al.*, 1991; Aranda-Olmedo *et al.*, 2002). Interestingly, there is not a REP downstream *phaZ* in *P. putida* KT2442, supporting the existence of the mRNA *phaC1ZC2D* transcribed from P_{C1} promoter in this strain. An additional role of REP sequences would be to allow the binding of DNA gyrase to relax DNA when excessive positive supercoiling is generated, especially between two convergent genes simultaneously transcribed (Liu and Wang, 1987; Wu *et al.*, 1988; Yang and Ames, 1988). In this sense, inverted REP sequences were found also downstream of *phaD* in *P. putida* GPo1 and KT2442 (Fig. 1), although the nucleotide sequence in this region is not identical in both strains (data not shown). Thus, REP sequences found between *phaD* and *phaF* genes could favour simultaneous transcription of *pha* genes, enabling the relaxation of supercoiled DNA in the intergenic region.

The different expression profiles of the transcription units *phaF* and *phaIF* were observed firstly in *P. putida* GPo1 (Prieto *et al.*, 1999) suggesting the possible presence of two promoters, one located upstream of the *phaI* gene and the other located upstream of *phaF*. A different expression of *phaF* and *phaIF* transcription units was also observed for *P. putida* KT2440 and *P. aeruginosa* (Hoffmann and Rehm, 2004; 2005; Rehm, 2006). In this study, we have demonstrated experimentally the existence and different expression profiles of these transcription units showing different activity in terms of transcription intensity and PhaD dependence.

The transcription regulators of the TetR family whose functions have been described so far for 85 out of more than 2300 proteins are usually repressors which are inactivated by small ligands such as antibiotics, drugs, catabolites, osmoprotectants and quorum-sensing autoinducers (Ramos *et al.*, 2005). One exception is the DhaS regulator, an activator of the *dha* operon in *Lacotococcus lactis* (Christen *et al.*, 2006). Similarly to PhaD (Figs 1 and 3), DhaS binds to an operator sequence partially overlapping the −35 promoter box (Christen *et al.*, 2006), whereas TetR-like repressors bind to inverted repeats that overlap or are located downstream of the −10 promoter box (Grkovic *et al.*, 1998). Few other TetR-type proteins have been suggested to activate gene expression; however, their mechanisms have not been described so far (Alatoom *et al.*, 2007; Chatterjee *et al.*, 2007; Audra *et al.*, 2008; Hirano *et al.*, 2008).

According to our results, binding to operator DNA sequences is a necessary, albeit not sufficient, requirement for PhaD to become an activator of *pha* gene expressions. In this sense, our data also demonstrate the need for PHA precursors (i.e. octanoate), or related intermediates of the fatty acid β-oxidation pathway for the complete transcription of the *pha* genes (Table 3 and Fig. S1). The 3D model of the PhaD structure that we have proposed appears to be compatible with the binding of such metabolic intermediates (Fig. 4). The most noteworthy feature of this model is the presence of a long deep crevice that may accommodate an extended HOCoA molecule without relevant steric hindrances (Fig. 4). Whereas the EthR effector-binding site is mainly hydrophobic to accommodate its hexadecyloctanoate ligand, many polar residues are found in the PhaD effector-pocket (Fig. S3), in accordance with the presence of a more polar ligand such as a CoA-intermediate of fatty acid β-oxidation.

Summarizing, our results have provided the first exhaustive experimental analysis of the complex transcription system that allows the simultaneous production of the PHA-related proteins to maintain the metabolic balance and polymer turnover in *P. putida* KT2442. In addition, we have demonstrated for the first time that PhaD regulator is directly involved in the transcriptional control of the *pha* cluster. Moreover, we have proved that PhaD is one of the few activators of the TetR-like family of regulators. Although the *pha* cluster is induced by octanoic acid, the 3D structural model of PhaD allowed us to propose that a CoA-derivative could be the true inducer. These findings allow us to conclude that PhaD represents a paradigmatic example within the whole scenario of bacterial regulators.

Experimental procedures

Bacterial strains, media and growth conditions

Pseudomonas putida KT2442 (Franklin *et al.*, 1981) is a derivative strain of the parental strain KT2440 whose complete nucleotide sequence is accessible in the data bank (Nelson *et al.*, 2002). *Pseudomonas putida* KT42C1 (de Eugenio *et al.*, 2010) is a PhaC1 mutant strain of *P. putida* KT2442 constructed via disruption of *phaC1* gene by insertion of a minitransposon containing kanamycin-resistance gene (de Lorenzo *et al.*, 1990; Herrero *et al.*, 1990). Unless otherwise stated, *Escherichia coli* and *P. putida* strains were grown in Luria–Bertani (LB) medium (Sambrook and Russell, 2001) at 37°C and 30°C respectively. The appropriate selection antibiotics, ampicillin (100 μg ml^{-1}), gentamicin (10 μg ml^{-1}), chloramphenicol (34 μg ml^{-1}) or kanamycin (50 μg ml^{-1}) were added when needed. For poly(hydroxyoctanoate-co-hydroxyhexanoate) [P(HO-*co*-HH)] production, *P. putida* strains were grown as previously described (de Eugenio *et al.*, 2010).

DNA and RNA manipulations

DNA manipulations and other Molecular Biology techniques were essentially performed as described previously

(Sambrook and Russell, 2001). Plasmid transference to the target *Pseudomonas* strains was done by the filter-mating technique (Herrero *et al*., 1990). DNA fragments were purified by standard procedures using Gene Clean (Bio 101, Vista, CA). For PCR amplification, we used two units of AmpliTaq DNA polymerase (PerkinElmer Life Sciences), 10 ngr of DNA template, 1 μg of each deoxynucleoside triphosphate and 2.5 mM $MgCl_2$ in the buffer recommended by the manufacturer. Conditions for amplification were chosen according to the G + C content of the corresponding oligonucleotides. Nucleotide sequences were determined directly with the same oligonucleotides used for cloning. Standard protocols of the manufacturer for *Taq* DNA polymerase-initiated cycle sequencing reactions with fluorescently labelled dideoxynucleotide terminators (Applied Biosystems) were used in an ABI Prism 3730 DNA Sequencer.

Construction of PhaD mutant

Pseudomonas putida KT42D strain was constructed by disruption of *phaD* gene using pK18*mob* plasmid (Schafer *et al*., 1994). An internal EcoRI/BamHI fragment of 384 bp of the gene was cloned in the polylinker of pK18*mob* after PCR amplification with primers D5mut (5′-CCGGAATTCCAAC GAACTCGGCATCAGC-3′) and D3mut (5′-CGGGATCCG ATCTGCTCGACCAGTTGCCC-3′). The resulting construction, pK18mob-mutd, was introduced into *P. putida* KT2442 by triparental mating using the strains *E. coli* DH10B (Invitrogen) and *E. coli* HB101 (pRK600) (de Lorenzo *et al*., 1990) as donor and helper strains respectively. Conjugants were selected in M63 0.2% citrate plus kanamycin. Disruption of *phaD* gene in the strain KT42D was confirmed by PCR sequencing analyses.

Plasmid constructions

The *phaD* coding sequence was amplified by PCR using oligonucleotides phaD5 (5′-CCCAAGGCTT**ATG**AAAACCC GCGATCGTATCC-3′) (the start codon is indicated in bold and an engineered HindIII site is underlined) and phaD3 (5′-CTAGTCTAGACTACCCCTCCAGGTACTTCACTGCC-3′) (XbaI site is underlined) and KT2442 genome as DNA template. The amplified DNA fragment was digested with HindIII and XbaI and then inserted into pIZ1016 vector (Moreno-Ruiz *et al*., 2003). The resulting recombinant plasmid was transformed into *E. coli* DH10B, *P. putida* KT2442 and *P. putida* KT42D.

Construction of lacZ *reporter* P. putida *KT2442 strains*

Upstream regions of each *pha* genes of 219–737 bp flanked by engineered EcoRI and BamHI sites were fused to the reporter gene *lacZ* of *E. coli* using pUJ9 plasmid (de Lorenzo *et al*., 1990) (Table 1). Reporter fusions were inserted into the chromosome of the target strains by the pUT-Km miniTn*5* delivery system by the filter-mating technique (Herrero *et al*., 1990), which allows the generation of reporter strains carrying translational fusions with the *lacZ* gene stably inserted into their chromosome. The selection of each reporter strain was made among three different candidates with similar expression levels to avoid promoter-unrelated *lacZ* expression. *E. coli* CC118*λpir* and *E. coli* HB101 (pRK600) were used as donor and helper strains, respectively, during the parental mating as previously described (de Lorenzo *et al*., 1990). Table 1 shows the details (region amplified, fragment size, primers used, plasmid construction and resulting reporter strain) of each construction. Correct insertion was tested by PCR technique. Isolated transconjugant strains grown at an OD_{600} of 0.2 were cultured in 0.1 N M63 medium plus 15 mM octanoic acid or 20 mM glucose. Three strains of each fusion selected did not show differences in terms of PHA content and growth profile on LB and 0.1 N M63 medium plus 15 mM octanoic acid or 20 mM glucose when compared with the wild-type strain.

Real-time PCR assay

Total RNA was extracted from *P. putida* KT2442 grown in 0.1 N M63 medium plus 15 mM octanoic acid or 20 mM glucose. For RNA purifications, 500 ml flasks containing 200 ml of culture medium were inoculated with overnight grown cells to reach an optical density (OD_{600}) of 0.3, and incubated at 30°C with shaking. Aliquots of 5 ml of cells were harvested throughout the growth curve (0, 3.5, 7 and 24 h) and stored at −20°C. Pellets were thawed and cells lysed in TE buffer (10 mM Tris-HCl pH 7.5, 1 mM EDTA) containing 5 mg of lysozyme per ml by a series of freeze/thaw cycles. RNA was extracted using the RNeasy mini kit (Qiagen), including a DNase I treatment according to the manufacturer's instructions, precipitated with ethanol, washed and resuspended in 40 μl of RNase-free water. The concentration and purity of the RNA samples were measured by using a ND1000 spectrophotometer (Nanodrop Technologies). Synthesis of total cDNA was carried out with 20 μl reverse transcription reactions containing 1 μg of RNA, 0.5 mM dNTPs, 200 U of SuperScript II Reverse Transcriptase (Invitrogen) and 5 μM of random hexamers as primers, in the buffer recommended by the manufacturer. Samples were initially heated at 65°C for 5 min and then incubated at 42°C for 1 h, terminated by incubation at 70°C for 15 min. The cDNA obtained was purified using Geneclean Turbo kit (MP Biomedicals) and the concentration was measured using a ND100 Spectrophotometer (Nanodrop Technologies). For the analysis of the transcripts levels target cDNAs (0.5 and 5 ng) and reference samples were amplified three times in separate PCR with 0.2 μM each of target primers by using the iQ5 Multicolor Real-Time PCR Detection System (Bio-Rad). Target primers were: primers C1RT5′ (5′-CTGGGCACCA GCGAAGGCG-3′) and C1RT3′ (5′-GTAATCGACAGCACC GCGTC-3′) for *phaC1*; C2RT5′ (5′-GCGGCGTGGCTCA CCTG-3′) and C2RT3′ (5′-GAAGCTGTTGGTCGCGCTG-3′) for *phaC2*; ZRT5′ (5′-GAAGTCATCGCCTTTGATGTGCC-3′) and ZRT3′ (5′-ATCATCCACAGCACCTTGGGCTTG-3′) for *phaZ*; D-RTf (5′-CATCAGCCCAGGCAACCTGTAC-3′) and D-RTr (5′-GCGCTCGACGATCAAGTGCAG-3′) for *phaD;* F-RTf (5′-GTCATGTTTAGACGGAATACCCAG-3′) and F-RTr (5′-GCGGCCAACCACCAGCTTG-3′) for *phaF*; I-RTf (5′-GC ACCGGTCAGCTTCTCGATC-3′) and I-RTr (5′-GGAGCGA ACTTGAAGAAGCC-3′) for *phaI.* Real-time PCR was performed using SYBR Green technology in an ABI Prism 7000 Sequence Detection System (Applied Biosystems). Samples

were initially denatured by heating at 95°C for 4 min, followed by 30 cycles of amplification (95°C, 1 min; test annealing temperature, 65°C, 1 min; elongation and signal acquisition, 72°C, 30 s). For quantification of the fluorescence values, a calibration curve was made using dilution series from 5.10^{-7} to 5 ng of *P. putida* KT2442 genomic DNA sample.

Gel retardation assays

P_{C1}, P_F and P_I DNA fragments (Table 1) used as probes were labelled at their 5′-end with phage T4 polynucleotide kinase and [α-^{32}P]-ATP (3000 Ci mmol^{-1}) (Amersham Biosciences). The DNA probes were purified by the QIAquick nucleotide removal kit (Qiagen). Reactions with increasing concentrations of crude extracts (0.08–3.5 μg of total protein) were performed as described elsewhere (Manso *et al*., 2009). The gels were dried onto Whatman 3MM paper and exposed to Hyperfilm MP (Amersham Biosciences).

Mapping transcription start sites

Pseudomonas putida KTpC1 and *P. putida* KTpI cells were grown in 0.1 N M63 medium with 15 mM octanoate during 7 h until the cultures reached an OD_{600} of about 2. Total RNA was isolated using the RNA/DNA Midi kit (Qiagen) according to the instructions of the supplier. Primer extension reactions were carried out with the avian myeloblastosis virus reverse transcriptase as described previously (Prieto and García, 1997), using LAC57 primer (5′-CGATTAAGTTGGGTAAC GCCAGGG-3′). To determine the length of the primer extension products, sequencing reactions of plasmids pUJC1 and pUJI (Table 1) were carried out with the same primer by using the T7 sequencing kit and [α-^{32}P]-dATP (Amersham Biosciences) as indicated by the supplier. Products were analysed on 6% polyacrylamide-urea gels. The gels were dried onto Whatman 3MM paper and exposed to Hyperfilm MP (Amersham Biosciences).

DNase I protection experiments

For DNase I footprinting experiments, the DNA fragments P_{C1}, and P_I were amplified by PCR with the target primers (Table 1) using 10 ng of plasmids pUJC1 and pUJI respectively (Table 1) as templates. Fragments were labelled using a combination of one unlabelled primer and a second primer end-labelled with phage T4 polynucleotide kinase [α-^{32}P]-ATP (111 TBq mmol^{-1}). Then the PCR fragment was purified using the High Pure PCR Product Purification kit from Boehringer Mannheim according to the manufacturer's instructions. Reactions with increasing concentrations of crude extracts (0.6–6 μg of total protein) were performed as described before (Galán *et al*., 2001). Protected bands were identified by comparison with the migration of the same fragment treated for the A+G sequencing reaction (Maxam and Gilbert, 1977).

Analytical procedures

Cell densities, expressed in grams of CDW per litre, were determined gravimetrically as described previously (de Eugenio *et al*., 2010).

For PHA content determination, about 5–10 mg of lyophilized cells was analysed following the procedure reported before (Lageveen *et al*., 1988). The P(HO-*co*-HH) was isolated from *P. putida* KT2442 cells as described in Lageveen and colleagues (1988).

Assay of β-galactosidase activity with whole *P. putida* cells was performed as described previously (Miller, 1972). It is worth to notice that the *P. putida* strains produced PHA at different rates under the assayed growth conditions using octanoate or glucose as carbon sources. Then, differences in the PHA cell content affect considerably to the turbidity measurement (de Eugenio *et al*., 2010) and consequently, the classical Miller method is not suitable for the determination of the β-galactosidase in a comparative and quantitative assay. β-Galactosidase activity assays in *P. putida* strains were performed as described previously, by considering one unit of β-galactosidase activity in *P. putida* strains is defined as 1 μmol of *o*-nitrophenyl-β-d-galactopyranoside hydrolysed per mg of residual biomass per min. Residual biomass is defined as PHA-free CDW (Prieto *et al*., 1999).

Homology modelling of PhaD

The 3D structure of PhaD was modelled using Swiss PDB Viewer 3.7 (Guex and Peitsch, 1997). The template used was the EthR regulator from *Mycobacterium tuberculosis* complexed with hexadecyloctanoate (PDB code 1U9N) (Frénois *et al*., 2004). Primary structure alignments were performed by the CLUSTALW utilities contained in the Network Protein Sequence Analysis server at http://npsa-pbil.ibcp.fr (Combet *et al*., 2000). In order to model the protein–ligand interaction, a PDB file of 3-hydroxyoctanoyl-coenzyme A was generated using the ChemOffice 8.0 utilities (CambridgeSoft) and manually docked onto the PhaD model in order to get the maximum overlap with the template ligand hexadecyloctanoate, using Swiss PDB viewer. Raw structures obtained from fitting were subsequently refined by steepest descent energy minimization and checked for packing errors and optimal bonding. Figures were rendered using the software package PyMol (Delano Scientific LLC).

Acknowledgements

We thank Dr E. Díaz for helpful discussions. The technical works of A. Valencia and V. Morales are greatly appreciated. This work was supported by grants from the Comunidad Autónoma de Madrid (P-AMB-259-0505), the Ministry of Science and Innovation (BIO2007-67304-C02, CSD2007-00005) and by European Union Grants (GEN 2006-27750-C5-3-E and NMP2-CT-2007-026515).

References

Alatoom, A., Aburto, R., Hamood, N., and Colmer-Hamood, A. (2007) VceR negatively regulates the *vceCAB* MDR efflux operon and positively regulates its own synthesis in *Vibrio cholerae* 569B. *Can J Microbiol* **53:** 888–900.

Aranda-Olmedo, I., Tobes, R., Manzanera, M., Ramos, J.L., and Marqués, S. (2002) Species-specific repetitive

extragenic palindromic (REP) sequences in *Pseudomonas putida*. *Nucleic Acids Res* **30:** 1826–1833.

Audra, P., Irgon, J., Berger, M., Bulyk, M., Wingreen, N., and Bassler, B. (2008) The *Vibrio harveyi* master quorum-sensing regulator, LuxR, a TetR-type protein is both an activator and a repressor: DNA recognition and binding specificity at target promoters. *Mol Microbiol* **70:** 76–88.

Castaneda, M., Guzman, J., Moreno, S., and Espin, G. (2000) The GacS sensor kinase regulates alginate and poly-beta-hydroxybutyrate production in *Azotobacter vinelandii*. *J Bacteriol* **182:** 2624–2628.

Chatterjee, A., Cui, Y., Hasegawa, H., and Chatterjee, A. (2007) PsrA, the *Pseudomonas* sigma regulator, controls regulators of epiphytic fitness, quorum sensing signals and plant interactions in *Pseudomonas syringae pv. tomato* strain DC3000. *Appl Environ Microbiol* **73:** 3684–3694.

Christen, S., Srinivas, A., Bähler, P., Zeller, A., Pridmore, D., Bieniossek, C., *et al.* (2006) Regulation of the *Dha* operon of *Lactococcus lactis*: a deviation from the rule followed by the TetR family of transcription regulators. *J Biol Chem* **281:** 23129–23137.

Combet, C., Blanchet, C., Geourjon, C., and Deléage, G. (2000) NPS@: network protein sequence analysis. *Trends Biochem Sci* **25:** 147–150.

Dias, J.M., Lemos, P.C., Serafim, L.S., Oliveira, C., Eiroa, M., Albuquerque, M.G., *et al.* (2006) Recent advances in polyhydroxyalkanoate production by mixed aerobic cultures: from the substrate to the final product. *Macromol Biosci* **6:** 885–906.

de Eugenio, L.I., García, P., Luengo, J.M., Sanz, J.M., San Román, J., García, J.L., and Prieto, M.A. (2007) Biochemical evidence that *phaZ* gene encodes a specific intracellular medium chain length polyhydroxyalkanoate depolymerase in *Pseudomonas putida* KT2442. Characterization of a paradigmatic enzyme. *J Biol Chem* **282:** 4951–4962.

de Eugenio, L.I., García, J.L., García, P., Prieto, M.A., and Sanz, J.M. (2008) Comparative analysis of the physiological and structural properties of a medium chain length polyhydroxyalkanoate depolymerase from *Pseudomonas putida* KT2442. *Eng Life Sci* **8:** 260–267.

de Eugenio, L.I., Escapa, I.F., Morales, V., Dinjaski, N., Galán, B., García, J.L., and Prieto, M.A. (2010) The turnover of medium-chain length polyhydroxyalkanoates in *Pseudomonas putida* KT2442 and the fundamental role of PhaZ depolymerase for the metabolic balance. *Environ Microbiol* **12:** 207–221.

Franklin, F.C., Bagdasarian, M., Bagdasarian, M.M., and Timmis, K.N. (1981) Molecular and functional analysis of the TOL plasmid pWWO from *Pseudomonas putida* and cloning of genes for the entire regulated aromatic ring meta cleavage pathway. *Proc Natl Acad Sci USA* **78:** 7458–7462.

Frénois, F., Engohang-Ndong, J., Locht, C., Baulard, A.R., and Villeret, V. (2004) Structure of EthR in a ligand bound conformation reveals therapeutic perspectives against tuberculosis. *Mol Cell* **16:** 301–307.

Galán, B., Kolb, A., García, J.L., and Prieto, M.A. (2001) Superimposed levels of regulation of the 4-hydroxyphenylacetate catabolic pathway in *Escherichia coli*. *J Biol Chem* **276:** 37060–37068.

Gavrilescu, M., and Chisti, Y. (2005) Biotechnology-a sustainable alternative for chemical industry. *Biotechnol Adv* **23:** 471–499.

Grkovic, S., Brown, H., Roberts, J., Paulsen, T., and Skurray, A. (1998) QacR is a repressor protein that regulates expression of the *Staphylococcus aureus* multidrug efflux pump QacA. *J Biol Chem* **273:** 18665–18673.

Guex, N., and Peitsch, C. (1997) SWISS-MODEL and the Swiss-PdbViewer: an environment for comparative protein modeling. *Electrophoresis* **18:** 2714–2723.

Herrero, M., de Lorenzo, V., and Timmis, K.N. (1990) Transposon vectors containing non-antibiotic resistance selection markers for cloning and stable chromosomal insertions of foreign genes in Gram negative bacteria. *J Bacteriol* **172:** 6557–6567.

Hirano, S., Tanaka, K., Ohnishi, Y., and Horinouchi, S. (2008) Conditionally positive effect of the TetR-family transcriptional regulator AtrA on streptomycin production by *Streptomyces griseus*. *Microbiology* **154:** 905–914.

Hoffmann, N., and Rehm, B.H. (2004) Regulation of polyhydroxyalkanoate biosynthesis in *Pseudomonas putida* and *Pseudomonas aeruginosa*. *FEMS Microbiol Lett* **237:** 1–7.

Hoffmann, N., and Rehm, B.H. (2005) Nitrogen-dependent regulation of medium-chain length polyhydroxyalkanoate biosynthesis genes in pseudomonads. *Biotechnol Lett* **27:** 279–282.

Huijberts, G.N., Eggink, G., de Waard, P., Huisman, G.W., and Witholt, B. (1992) *Pseudomonas putida* KT2442 cultivated on glucose accumulates poly(3-hydroxyalkanoates) consisting of saturated and unsaturated monomers. *Appl Environ Microbiol* **58:** 536–544.

Huisman, G.W. (1991) Poly(3-hydroxyalkanoates) from *Pseudomonas putida:* from DNA to plastic. PhD Thesis. Swiss Federal Institute of Technology Zurich.

Huisman, G.W., Wonink, E., Meima, R., Kazemier, B., Terpstra, P., and Witholt, B. (1991) Metabolism of poly(3-hydroxyalkanoates) (PHAs) by *Pseudomonas oleovorans*. Identification and sequences of genes and function of the encoded proteins in the synthesis and degradation of PHA. *J Biol Chem* **266:** 2191–2198.

Kessler, B., and Witholt, B. (2001) Factors involved in the regulatory network of polyhydroxyalkanoate metabolism. *J Biotechnol* **86:** 97–104.

Klinke, S., de Roo, G., Witholt, B., and Kessler, B. (2000) Role of *phaD* in accumulation of medium-chain-length poly(3-hydroxyalkanoates) in *Pseudomonas oleovorans*. *Appl Environ Microbiol* **66:** 3705–3710.

Laemmli, U.K. (1970) Cleavage of structural proteins during the assembly of the head of bacteriophage T4. *Nature* **227:** 680–685.

Lageveen, R.G., Huisman, G.W., Preusting, H., Ketelaar, P., Eggink, G., and Witholt, B. (1988) Formation of polyesters by *Pseudomonas oleovorans*: effect of substrates on formation and composition of poly-(R)-3-hydroxyalkanoates and poly-(R)-3-hydroxyalkenoates. *Appl Environ Microbiol* **54:** 2924–2932.

Liu, L.F., and Wang, J.C. (1987) Supercoiling of the DNA template during transcription. *Proc Natl Acad Sci USA* **84:** 7024–7027.

de Lorenzo, V., Herrero, M., Jakubzik, U., and Timmis, K.N. (1990) Mini-Tn*5* transposon derivatives for insertion

mutagenesis, promoter probing, and chromosomal insertion of cloned DNA in gram-negative eubacteria. *J Bacteriol* **172:** 6568–6572.

Luengo, J.M., García, B., Sandoval, A., Naharro, G., and Olivera, E. (2003) Bioplastics from microorganisms. *Curr Opin Microbiol* **6:** 251–260.

Madison, L.L., and Huisman, G.W. (1999) Metabolic engineering of poly(3-hydroxyalkanoates): from DNA to plastic. *Microbiol Mol Biol Rev* **63:** 21–53.

Manso, I., Torres, B., Andreu, J.M., Menéndez, M., Rivas, G., Alfonso, C., *et al.* (2009) 3-Hydroxyphenylpropionate and phenylpropionate are synergistic activators of the MhpR transcriptional regulator from *Escherichia coli*. *J Biol Chem* **284:** 21218–21228.

Maxam, M., and Gilbert, W. (1977) A new method for sequencing DNA. *Proc Natl Acad Sci USA* **74:** 560–564.

Miller, J.H. (1972) *Experiments in Molecular Genetics*. Cold Spring Harbor, NY, USA: Cold Spring Harbor Laboratory.

Moldes, C., García, P., García, J.L., and Prieto, M.A. (2004) *In Vivo* immobilization of fusion proteins on bioplastics by the novel tag BioF. *Appl Environ Microbiol* **70:** 3205–3212.

Moreno-Ruiz, E., Hernáez, M.J., Martínez-Perez, O., and Santero, E. (2003) Identification and functional characterization of *Sphingomonas macrogolitabida* strain TFA genes involved in the first two steps of the tetralin catabolic pathway. *J Bacteriol* **185:** 2026–2030.

Nelson, K.E., Weinel, C., Paulsen, I.T., Dodson, R.J., Hilbert, H., Martins dos Santos, V.A.P., *et al.* (2002) Complete genome sequence and comparative analysis of the metabolically versatile *Pseudomonas putida* KT2440. *Environ Microbiol* **4:** 799–808.

Premkumar, L., Rife, C.L., Sri Krishna, S., McMullan, D., Miller, M.D., Abdubek, P., *et al.* (2007) Crystal structure of TM1030 from *Thermotoga maritima* at 2.3 A resolution reveals molecular details of its transcription repressor function. *Proteins* **68:** 418–424.

Prieto, M.A., and García, J.L. (1997) Identification of a novel positive regulator of the 4-hydroxyphenylacetate catabolic pathway of *Escherichia coli*. *Biochem Biophys Res Commun* **232:** 759–765.

Prieto, M.A., Buhler, B., Jung, K., Witholt, B., and Kessler, B. (1999) PhaF, a polyhydroxyalkanoate-granule-associated protein of *Pseudomonas oleovorans* GPo1 involved in the regulatory expression system for *pha* genes. *J Bacteriol* **181:** 858–868.

Prieto, M.A., de Eugenio, L.I., Galán, B., Luengo, J.M., and Witholt, B. (2007) Synthesis and degradation of polyhydroxyalkanoates. In *Pseudomonas: A Model System in Biology. Pseudomonas*, Vol. V. Ramos, J.L., and Filloux, A. (eds). Berlin, Germany: Springer, pp. 397–428.

Rajan, S.S., Yang, X., Shuvalova, L., Collart, F., and Anderson, W.F. (2006) Crystal structure of YfiR, an unusual TetR/CamR-type putative transcriptional regulator from *Bacillus subtilis*. *Proteins* **65:** 255–257.

Ramos, J.L., Martínez-Bueno, M., Molina-Henares, A.J., Terán, W., Watanabe, K., Zhang, X., *et al.* (2005) The TetR family of transcriptional repressors. *Microbiol Mol Biol Rev* **69:** 326–356.

Rehm, B.H. (2006) Genetics and biochemistry of polyhydroxyalkanoate granule self-assembly: the key role of polyester synthases. *Biotechnol Lett* **28:** 207–213.

Rehm, B.H., Kruger, N., and Steinbüchel, A. (1998) A new metabolic link between fatty acid de novo synthesis and polyhydroxyalkanoic acid synthesis. The *phaG* gene from *Pseudomonas putida* KT2440 encodes a 3-hydroxyacyl-acyl carrier protein-coenzyme A transferase. *J Biol Chem* **273:** 24044–24051.

Ren, Q., de Roo, G., Ruth, K., Witholt, B., Zinn, M., and Thöny-Meyer, L. (2009) Simultaneous accumulation and degradation of polyhydroxyalkanoates: futile cycle or clever regulation? *Biomacromolecules* **10:** 916–922.

Ruth, K., de Roo, G., Egli, T., and Ren, Q. (2008) Identification of two Acyl-CoA synthetases from *Pseudomonas putida* GPo1: one is located at the surface of polyhydroxyalkanoates granules. *Biomacromolecules* **9:** 1652–1659.

Sambrook, J., and Russell, D.W. (2001) *Molecular Cloning. A Laboratory Manual*. Cold Spring Harbor, NY, USA: CSHL Press.

Sandoval, A., Arias-Barrau, E., Arcos, M., Naharro, G., Olivera, E.R., and Luengo, J.M. (2007) Genetic and ultrastructural analysis of different mutants of *Pseudomonas putida* affected in the poly-3-hydroxy-n-alkanoate gene cluster. *Environ Microbiol* **9:** 737–751.

Schafer, A., Tauch, A., Jager, W., Kalinowski, J., Thierbach, G., and Puhler, A. (1994) Small mobilizable multi-purpose cloning vectors derived from the *Escherichia coli* plasmids pK18 and pK19: selection of defined deletions in the chromosome of *Corynebacterium glutamicum*. *Gene* **145:** 69–73.

Schirmer, A., and Jendrossek, D. (1994) Molecular characterization of the extracellular poly(3-hydroxyoctanoic acid) [P(3HO)] depolymerase gene of *Pseudomonas fluorescens* GK13 and of its gene product. *J Bacteriol* **176:** 7065–7073.

Schumacher, M.A., Miller, M.C., Grkovic, S., Brown, M.H., Skurray, R.A., and Brennan, R.G. (2001) Structural mechanisms of QacR induction and multidrug recognition. *Science* **294:** 2158–2163.

Schumacher, M.A., Miller, M.C., Grkovic, S., Brown, M.H., Skurray, R.A., and Brennan, R.G. (2002) Structural basis for cooperative DNA binding by two dimers of the multidrug-binding protein QacR. *EMBO J* **21:** 1210–1218.

Sierro, N. (2005) Bi-functionality of the PhaF protein of *Pseudomonas putida* in the polyhydroxyalkanoate production process. PhD Thesis. Swiss Federal Institute of Technology Zurich.

Solaiman, D.K., Ashby, R.D., Licciardello, G., and Catara, V. (2008) Genetic organization of *pha* gene locus affects *phaC* expression, poly(hydroxyalkanoate) composition and granule morphology in *Pseudomonas corrugata*. *J Ind Microbiol Biotechnol* **35:** 111–120.

Timm, A., and Steinbüchel, A. (1992) Cloning and molecular analysis of the poly(3-hydroxyalkanoic acid) gene locus of *Pseudomonas aeruginosa* PAO1. *Eur J Biochem* **209:** 15–30.

Wu, H.Y., Shyy, S.H., Wang, J.C., and Liu, L.F. (1988) Transcription generates positively and negatively supercoiled domains in the template. *Cell* **53:** 433–440.

Yang, Y., and Ames, G.F. (1988) DNA gyrase binds to the family of prokaryotic repetitive extragenic palindromic sequences. *Proc Natl Acad Sci USA* **85:** 8850–8854.

Supporting information

Additional Supporting Information may be found in the online version of this article:

Fig. S1. Quantification of the expression rates of the *pha* genes by real-time RT-PCR assays. Gene transcription profiles of *pha* genes throughout growth of *P. putida* KT2442 (A–F), KT42C1 (G–L) and KT42D (M–Q) in M63 0.1 N plus 15 mM sodium octanoate (black bars) or 20 mM glucose (red bars) are shown; samples along the growth curve were taken at 0, 3.5, 7 and 23 h. The gene transcription of *phaC1* (A, G, M), *phaZ* (B, H, N), *phaC2* (C, I, O), *phaD* (D, J), *phaF* (E, K, P) and *phaI* (F, L, Q) genes is depicted. An initial concentration of 5 ng cDNA was used for quantitative RT-PCR. Error bars represent standard deviation calculated from the results of three independent experiments. *y*-axis: transcription level (cDNA ng); *x*-axis: time of culture (h).

Fig. S2. Gel retardation analyses of PhaD binding to the P_I, P_{C1} and P_F promoter regions.

A. The DNA probes used (P_I, P_{C1} and P_F) are indicated schematically on the right. Cell extract and gel retardation analyses were performed as described under *Experimental procedures*. Lanes 2–7 contained 0.086, 0.17, 0.34, 0.69, 1.7 and 3.4 μg of total protein of PhaD$^+$ extracts obtained from cells bearing plasmid pIZD (*phaD*) respectively. Lane 1 contained no extract and lane 8 contains 3.4 μg of total protein of PhaD-free extracts obtained from cells bearing control plasmid pIZ1016 respectively. The DNA–PhaD complexes are indicated.

B. PhaD binding competition analysis to P_I promoter with unlabelled DNA-specific probe (lanes 3, 4, 5) and unrelated salmon sperm DNA (lanes 6, 7, 8). Gel retardation was performed in the presence of 1.7 μg of total protein of PhaD$^+$ extracts. Lane 1 contains no extract.

Fig. S3. Homology-based 3D model of dimeric PhaD. A view of the most representative predicted polar interactions between HOCoA and PhaD. Colour scheme is CPK, with the exception of carbon atoms from the protein (green) or from the ligand (magenta). Oval highlights the 3-hydroxyoctanoyl moiety.

Please note: Wiley-Blackwell are not responsible for the content or functionality of any supporting materials supplied by the authors. Any queries (other than missing material) should be directed to the corresponding author for the article.

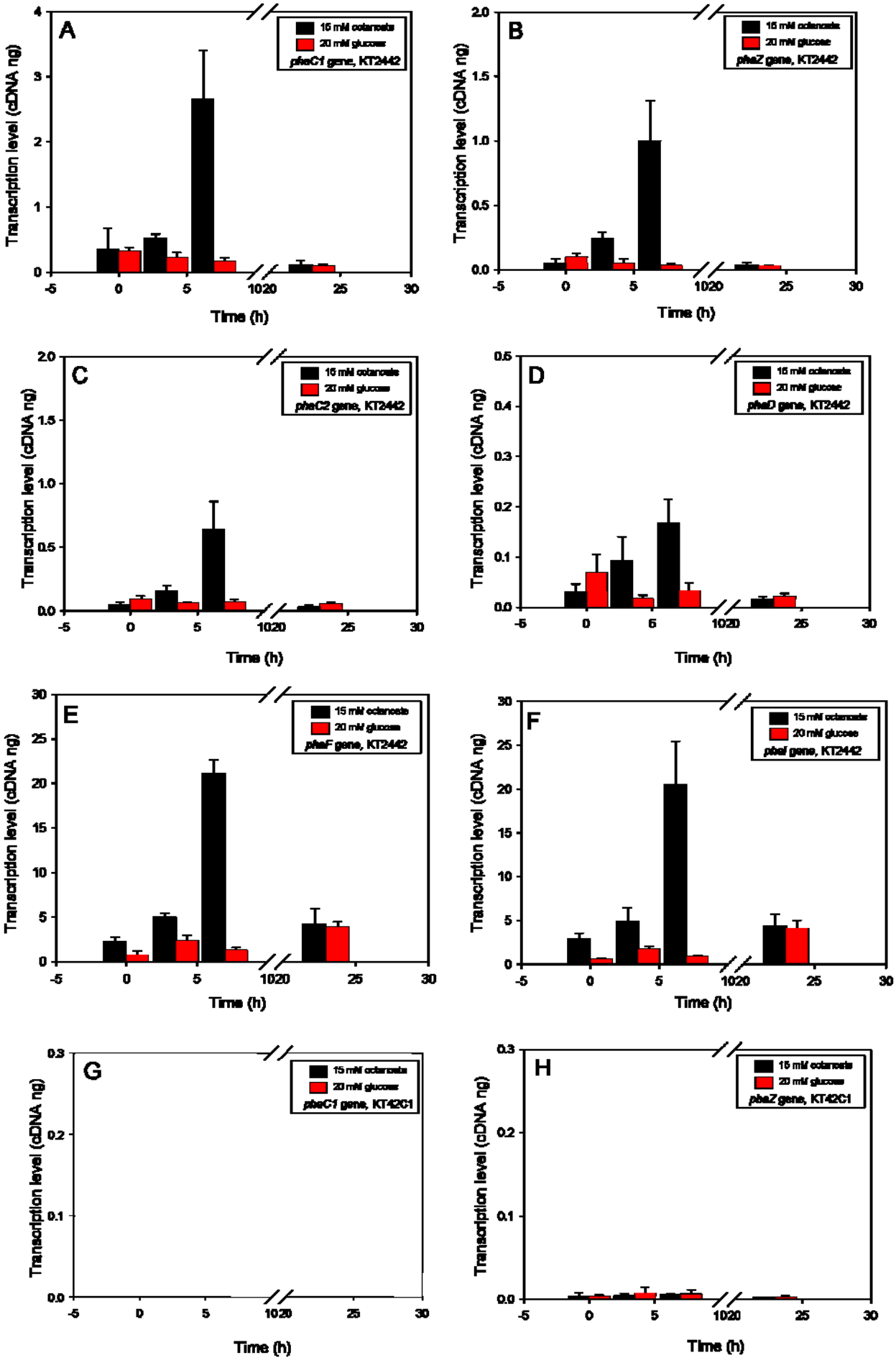
A
15 mM octanoate
20 mM glucose
phaC1 gene, KT2442
Transcription level (cDNA ng)
Time (h)
B
15 mM octanoate
20 mM glucose
phaZ gene, KT2442
Transcription level (cDNA ng)
Time (h)
C
15 mM octanoate
20 mM glucose
phaC2 gene, KT2442
Transcription level (cDNA ng)
Time (h)
D
15 mM octanoate
20 mM glucose
phaD gene, KT2442
Transcription level (cDNA ng)
Time (h)
E
15 mM octanoate
20 mM glucose
phaF gene, KT2442
Transcription level (cDNA ng)
Time (h)
F
15 mM octanoate
20 mM glucose
phaI gene, KT2442
Transcription level (cDNA ng)
Time (h)
G
15 mM octanoate
20 mM glucose
phaC1 gene, KT42C1
Transcription level (cDNA ng)
Time (h)
H
15 mM octanoate
20 mM glucose
phaZ gene, KT42C1
Transcription level (cDNA ng)
Time (h)

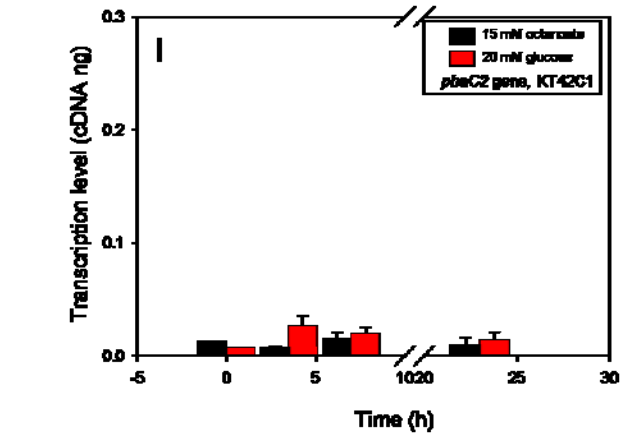
I
15 mM octanoate
20 mM glucose
phaC2 gene, KT42C1
Transcription level (cDNA ng)
Time (h)

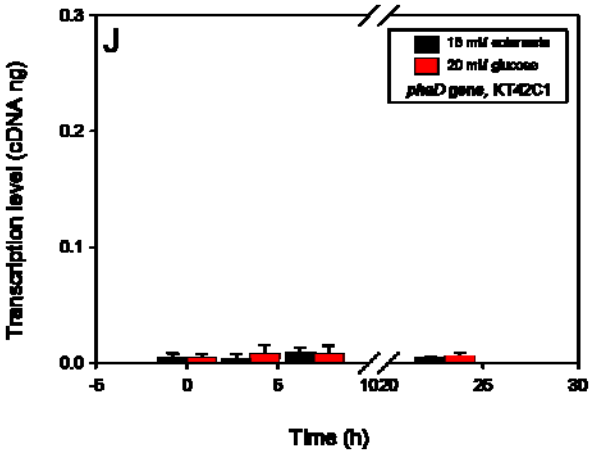
J
15 mM octanoate
20 mM glucose
phaD gene, KT42C1
Transcription level (cDNA ng)
Time (h)

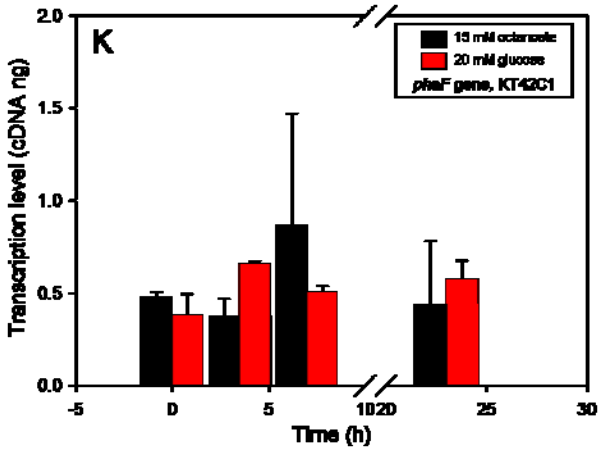
K
15 mM octanoate
20 mM glucose
phaF gene, KT42C1
Transcription level (cDNA ng)
Time (h)

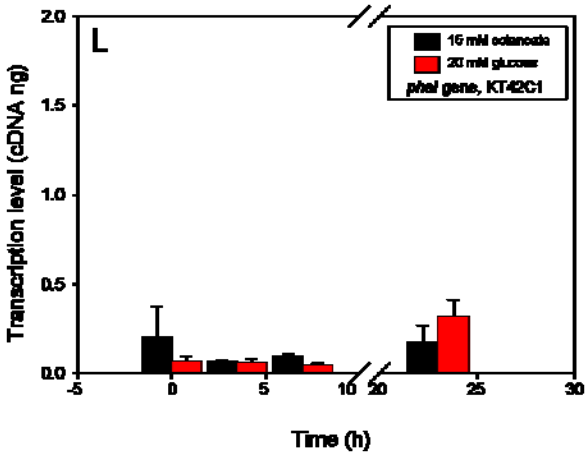
L
15 mM octanoate
20 mM glucose
phaI gene, KT42C1
Transcription level (cDNA ng)
Time (h)

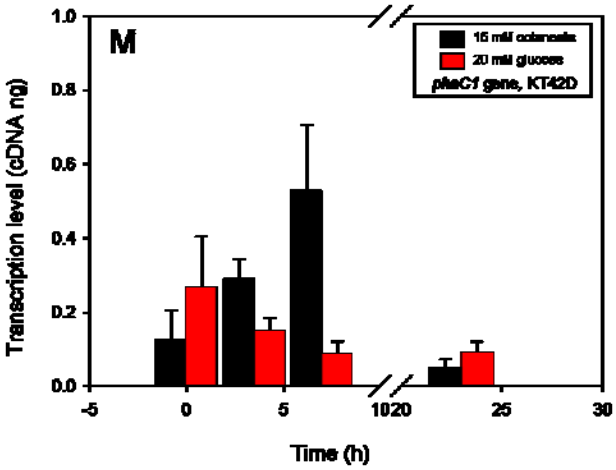
M
15 mM octanoate
20 mM glucose
phaC1 gene, KT42D
Transcription level (cDNA ng)
Time (h)

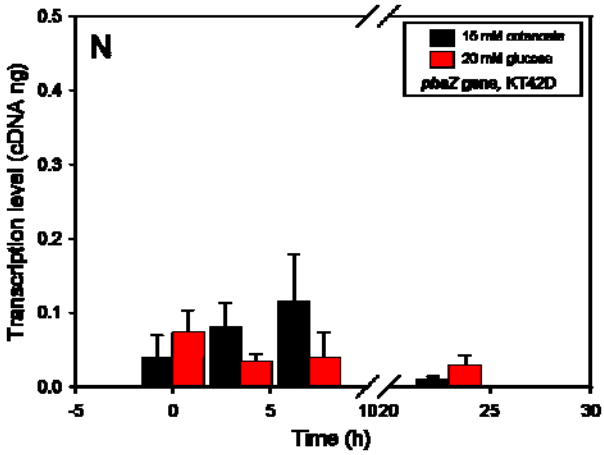
N
15 mM octanoate
20 mM glucose
phaZ gene, KT42D
Transcription level (cDNA ng)
Time (h)

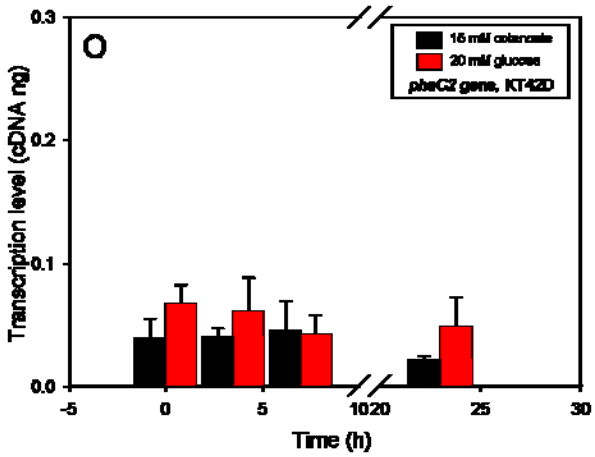
O
15 mM octanoate
20 mM glucose
phaC2 gene, KT42D
Transcription level (cDNA ng)
Time (h)

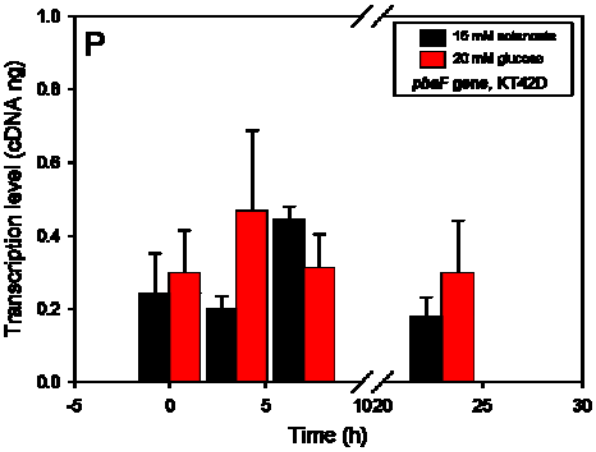
P
15 mM octanoate
20 mM glucose
phaF gene, KT42D
Transcription level (cDNA ng)
Time (h)

Fig. S2

A

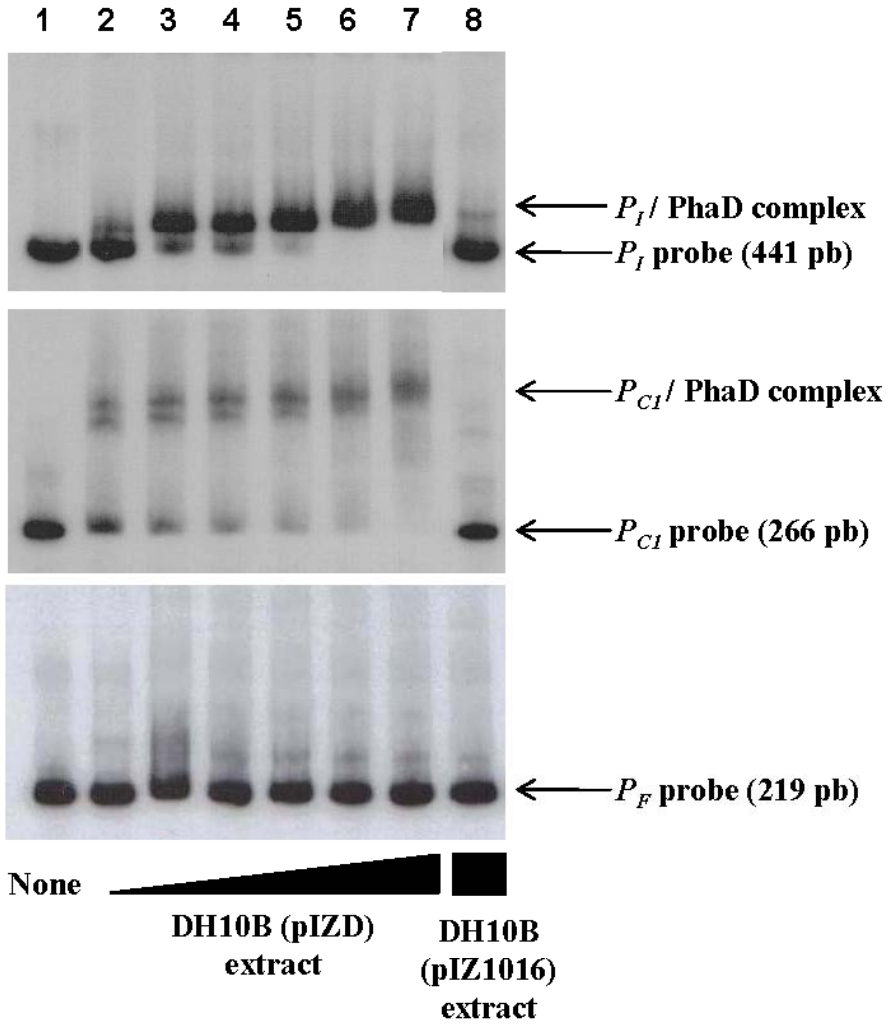
1 2 3 4 5 6 7 8
P_I/ PhaD complex
P_I probe (441 pb)
P_{C1}/ PhaD complex
P_{C1} probe (266 pb)
P_F probe (219 pb)
None
DH10B (pIZD) extract
DH10B (pIZ1016) extract

Fig. S2

B

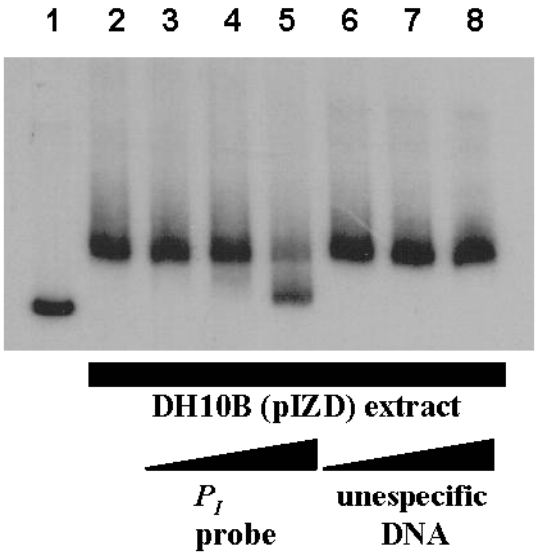

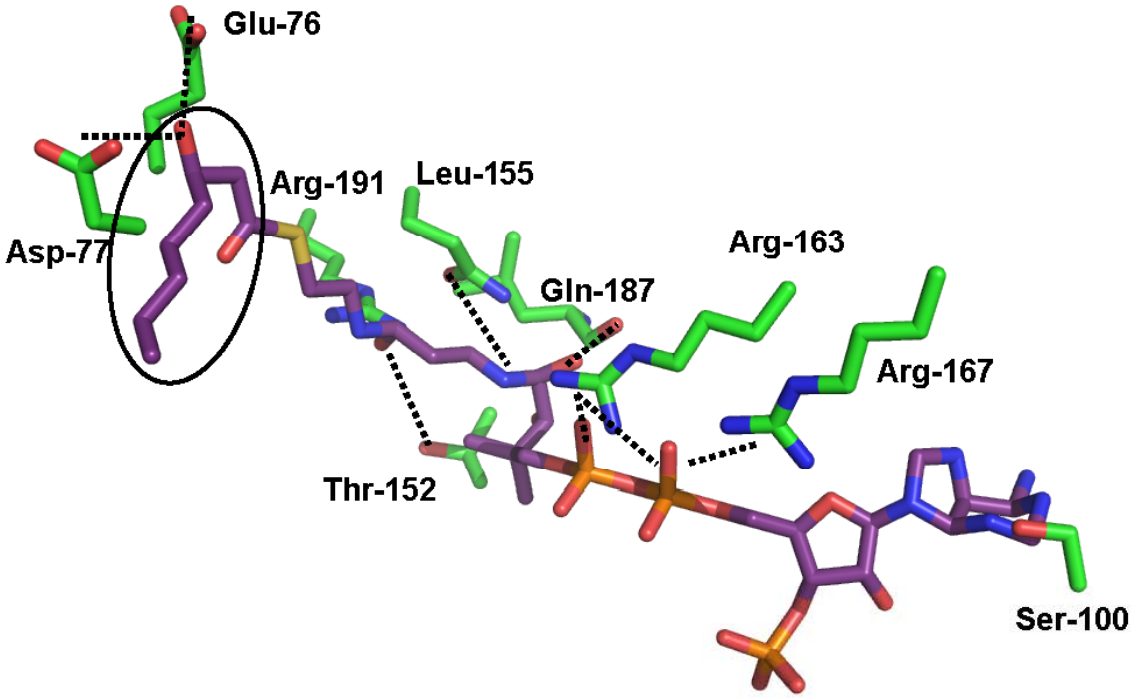
Glu-76
Asp-77
Arg-191
Leu-155
Arg-163
Gln-187
Arg-167
Thr-152
Ser-100

Figure S3

SUPPLEMENTAL INFORMATION

Fig. S1. Quantification of the expression rates of the pha genes by real-time RT-PCR assays. Gene transcription profiles of pha genes throughout growth of P. putida KT2442 (A–F), KT42C1 (G–L) and KT42D (M–Q) in M63 0.1 N plus 15 mM sodium octanoate (black bars) or 20 mM glucose (red bars) are shown; samples along the growth curve were taken at 0, 3.5, 7 and 23 h. The gene transcription of phaC1 (A, G, M), phaZ (B, H, N), phaC2 (C, I, O), phaD (D, J), phaF (E, K, P) and phaI (F, L, Q) genes is depicted. An initial concentration of 5 ng cDNA was used for quantitative RT-PCR. Error bars represent standard deviation calculated from the results of three independent experiments. y-axis: transcription level (cDNA ng); x-axis: time of culture (h).

Fig. S2. Gel retardation analyses of PhaD binding to the PI, PC1 and PF promoter regions.

A. The DNA probes used (PI, PC1 and PF) are indicated schematically on the right. Cell extract and gel retardation analyses were performed as described under Experimental procedures. Lanes 2–7 contained 0.086, 0.17, 0.34, 0.69, 1.7 and 3.4 μg of total protein of PhaD+ extracts obtained from cells bearing plasmid pIZD (phaD) respectively. Lane 1 contained no extract and lane 8 contains 3.4 μg of total protein of PhaD-free extracts obtained from cells bearing control plasmid pIZ1016 respectively. The DNA–PhaD complexes are indicated.

B. PhaD binding competition analysis to PI promoter with unlabelled DNA-specific probe (lanes 3, 4, 5) and unrelated salmon sperm DNA (lanes 6, 7, 8). Gel retardation was performed in the presence of 1.7 μg of total protein of PhaD+ extracts. Lane 1 contains no extract.

Fig. S3. Homology-based 3D model of dimeric PhaD. A view of the most representative predicted polar interactions between HOCoA and PhaD. Colour scheme is CPK, with the exception of carbon atoms from the protein (green) or from the ligand (magenta). Oval highlights the 3-hydroxyoctanoyl moiety.